Imaging and gene editing approaches highlight important role of autophagy in controlling *Mtb* infection.

Tuberculosis (TB) is a potentially lethal airborne disease caused by *Mycobacterium tuberculosis (Mtb)*. Last year, over 10.6 million people fell ill with TB worldwide and over 1.6 million lost their lives. The disease usually affects the lungs of infected individuals and leads to severe coughing, fever, and chest pains. Macrophages are the primary host cells for Mtb during its intracellular survival in humans.

Although effective treatments are available against *Mtb*, the standard treatment typically requires six months of antibiotics and depending on the drug susceptibility of the infecting strain, treatment sometimes lasts much longer. There is therefore an urgent need to uncover novel ways to treat TB without reliance on current antibiotic strategies.

It has been suggested that two autophagy pathways – the canonical (xenophagy) and non-canonical (LC3-associated phagocytosis; LAP) pathways – play a role in the response of host macrophages to *Mtb* infection. However, it has not previously been feasible to use gene deletion approaches to study the role of autophagy in primary human macrophages and it is unclear how these pathways control *Mtb* infection in phagosomes and the cytosol.

To address this, researchers at The Francis Crick Institute used a combination of CRISPR-Cas9 gene editing and high-content imaging approaches to investigate the role of autophagy in controlling *Mtb* infection.[1] Here, we explore how they developed their human macrophage cell model and investigated the roles of two autophagy proteins, ATG7 and ATG14, in bacterial replication and cell death.

Publication author

Max Gutierrez
Head of the Host-Pathogen Interactions in Tuberculosis Laboratory at The Francis Crick Institute

"For this study, it has been critical to use a system like the Opera Phenix that allows high-content live cell imaging to monitor tuberculosis infection in real time. Human macrophages display a very high phenotypic heterogeneity and being able to analyze thousands of cells per condition was very important to produce meaningful data. As *M. tuberculosis* is a CL3 human pathogen, these studies were performed with the Opera Phenix in a BSL3 facility, and this system facilitated the capture and acquisition of very large datasets with multicolor images."

Methods and results

Monitoring replication of *Mtb* in ATG7 and ATG14 KO iPSDMs

To investigate canonical and non-canonical autophagy responses to *Mtb* infection, Aylan et al. used CRISPR-Cas9 to knock out either *ATG7* or *ATG14* in induced pluripotent stem cell-derived macrophages (iPSDMs). They then used the Opera Phenix® high-content screening system to monitor the replication of wild-type and mutant *Mtb* strains expressing a fluorescent protein in the edited macrophages.

Two mutant *Mtb* strains were used in the study: one lacking both EsxA and EsxB (*Mtb* Δ*esxBA*), two substrates responsible for phagosome damage and induction of xenophagy, and another lacking CpsA (*Mtb* Δ*cpsA*), which is reported to be unable to block LAP in macrophages. The strains were therefore unable to trigger canonical autophagy (*Mtb* Δ*esxBA*) or unable to block non-canonical autophagy (*Mtb* Δ*cpsA*), and both showed reduced replication after infection of unedited iPSDMs.

Single-cell high-content imaging revealed that deletion of *ATG7* resulted in increased replication of wild-type *Mtb*, but not of the mutant *Mtb* strains in iPSDMs after infection (Figure 1a-f). During the analysis, the team noticed that in macrophages infected with wild-type *Mtb*, there was a reduction in the total number of cells analyzed by high-content imaging. To investigate whether this was related to cell death, they stained the infected cells with a reagent that selectively stains cells with compromised plasma membrane integrity. They observed that the percentage of dead cells in ATG7 KO was significantly higher than wild-type ($ATG7^{+/+}$) iPSDMs after infection with wild-type *Mtb*, indicating that in ATG7 KO cells, the infection was associated with macrophage cell death (Figure 1g, h).

The deletion of *ATG14*, which only disrupts canonical autophagy and leaves non-canonical autophagy intact, led to a more pronounced increased replication of wild-type *Mtb* at 96 hours post-infection. Notably, the mutant *Mtb* Δ*esxBA* also showed increased replication, while the *Mtb* Δ*cpsA* mutant was still restricted. The authors believe this indicates that ATG14 is required to control the replication of wild-type *Mtb* and the Δ*esxBA* mutant.

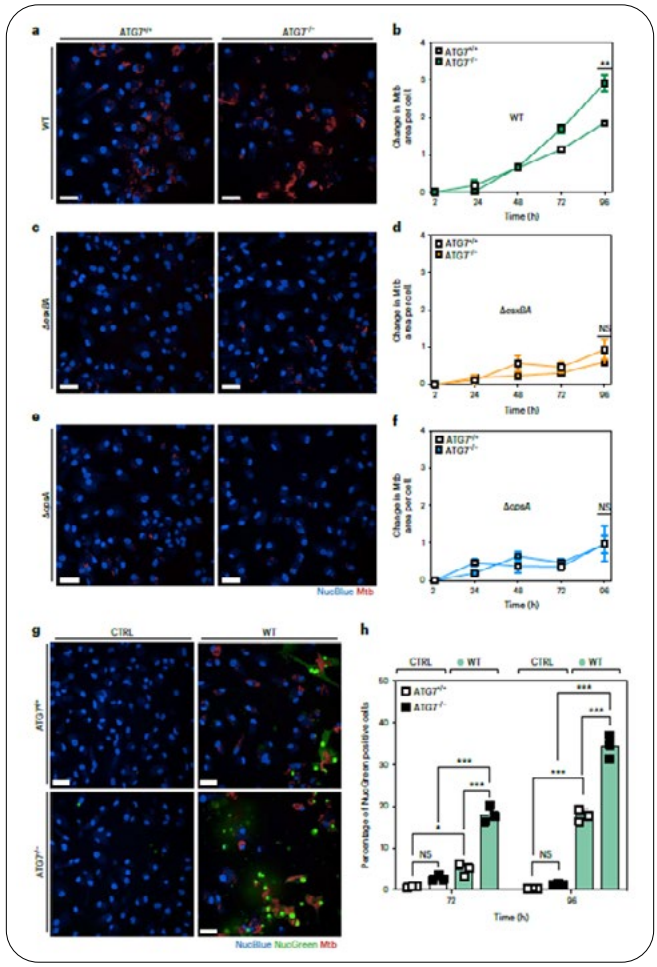

Figure 1: Increased *Mtb* replication in ATG7-deficient iPSDM. a,c,e) Snapshot of live $ATG7^{+/+}$ and $ATG7^{-/-}$ iPSDM infected with *Mtb* WT, Δ*esxBA*, and Δ*cpsA* at 96 h. Nuclear staining (blue) and *Mtb*-E2-Crimson (red). Scale bars, 50 µm. b,d,f) High-content quantitative analysis of *Mtb* replication after infection of $ATG7^{+/+}$ or $ATG7^{-/-}$ iPSDM with *Mtb* WT, Δ*esxBA*, and Δ*cpsA*. *Mtb* area per cell was calculated as fold change, relative to 2 h post-infection. Data representative from one out of two independent experiments (n = 3 independent wells). Results are shown as mean ± s.e.m. An unpaired two-tailed t-test was used for comparisons $^{**}P < 0.002$; NS, non-significant. G) Representative images of Blue/Green (Live/Dead)-stained $ATG7^{+/+}$ and $ATG7^{-/-}$ iPSDM uninfected (CTRL) or infected with *Mtb* WT for 96 h. Nuclear staining (blue) and dead nuclear staining (green). Scale bars, 50 µm. h) Quantitative analysis of the percentage of NucGreen-positive cells in each condition. Data representative from one out of two independent experiments (n = 3 independent wells). Results are shown as mean ± s.e.m. One-way ANOVA followed with Šídák's multiple comparison test. $^{***}P < 0.001$, $^{*}P < 0.033$; NS, nonsignificant. Image credit: Aylan, Bernard, Pellegrino, et al., 2023

When they investigated whether the increase in replication was related to cell death, they found an increase in the number of dead cells in ATG14 KO iPSDMs infected with wild-type *Mtb*, but not with the two mutant strains.

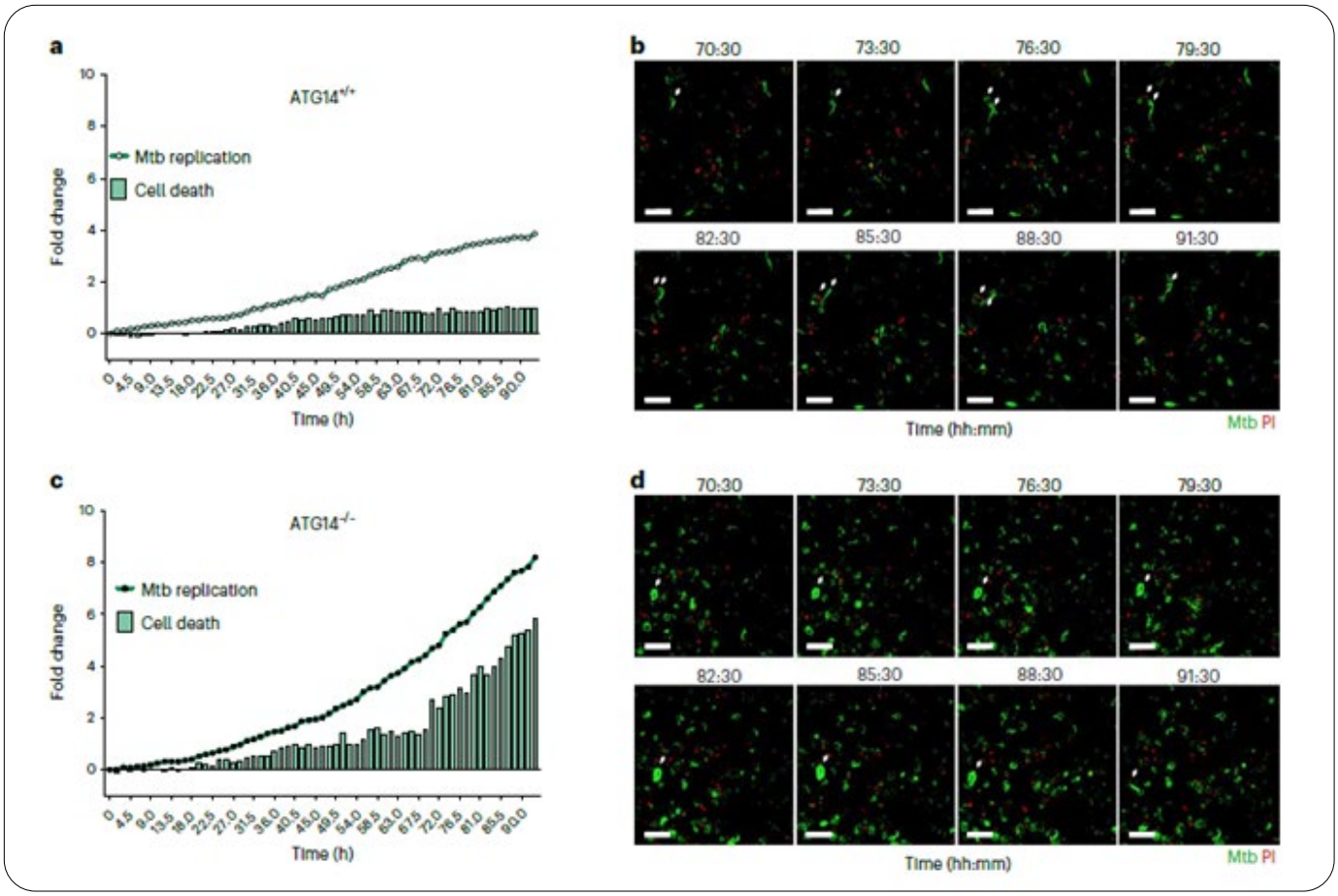

Figure 2: Unrestrained *Mtb* replication and cell death in ATG14-deficient cells. a,c) High-content quantitative analysis of live *Mtb* WT replication in ATG14$^{+/+}$ (a) or ATG14$^{-/-}$ (c) iPSDM. *Mtb* area (dot plot) and cell death (bar plot) were calculated as fold change, relative to *Mtb* uptake at time 0 h post-infection. Data representative from one out of two independent experiments. b,d) Representative micrographs at indicated time points of ATG14$^{+/+}$ (b) or ATG14$^{-/-}$ (d) iPSDM infected with *Mtb* WT (green) in the presence of PI (red). Data representative from one out of two independent experiments. Scale bars, 50 µm.
Image credit: Aylan, Bernard, Pellegrino, et al., 2023

Investigating ATG14 KO iPSDM cell death using live-cell imaging

To determine whether the ATG14 KO iPSDMs were dying because of high bacterial burden or whether increased *Mtb* replication happened after they underwent cell death, the team performed high-content live-cell imaging of iPSDMs infected with wild-type *Mtb* in the presence of propidium iodide (PI), a probe for the loss of plasma membrane integrity. Although *Mtb* replication was higher in ATG14 KO iPSDMs from 48 hours onwards, an increase in cell death was only observed from 72 hours, suggesting that enhanced *Mtb* replication precedes cell death (Figure 2). Bacterial replication continued after cells became leaky, and most of the cells with increased bacterial load were compromised.

Understanding increased *Mtb* replication in ATG14 KO iPSDMs

To explore whether the increased replication of wild-type *Mtb* was due to enhanced cytosolic access, the researchers used Galectin-3 (Gal3) as a marker, which is known to recognize luminal glycans of damaged phagosomal membranes. Using high-content imaging and analysis they observed that the percentage of Gal3-positive phagosomes containing wild-type *Mtb* and *Mtb* Δ*cpsA* was higher in ATG14 KO compared with wild-type iPSDMs just 2 hours after infection (Figure 3). Because this effect was observed at the early stages of infection, the authors predict that ATG14 regulates early access of *Mtb* to the cytosol. These findings were also confirmed by transmission electron microscopy (TEM), where a higher percentage of wild-type *Mtb* were localized in the cytosol of ATG14 KO iPSDMs 48 hours after infection.

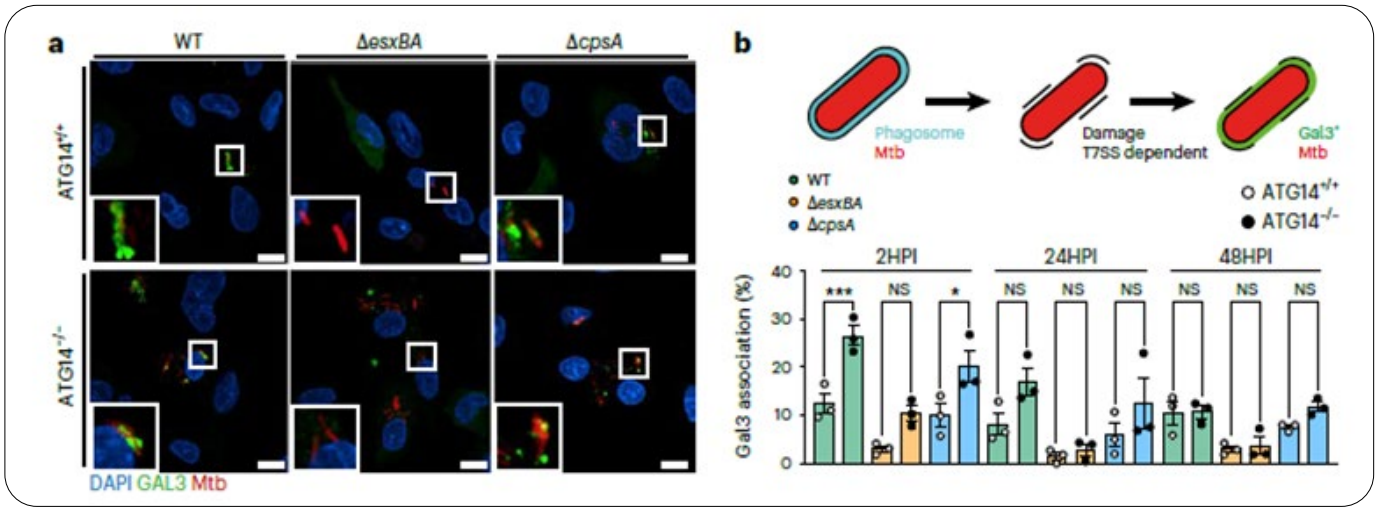

Figure 3: ATG14 contributes to the maintenance of *Mtb* in phagosomes. a) GAL3 staining in ATG14$^{+/+}$ or ATG14$^{-/-}$ iPSDM infected with *Mtb* WT, Δ*esxBA*, or Δ*cpsA*. Nuclear staining (blue), GAL3 (green), and *Mtb* E2-Crimson (red). Scale bars, 10 µm. b) Compiled data from three independent experiments. Results are shown as mean ± s.e.m. One-way ANOVA followed with Šídák's multiple comparison test. ***P < 0.001, **P < 0.002; NS, non-significant.
Image credit: Aylan, Bernard, Pellegrino, et al., 2023

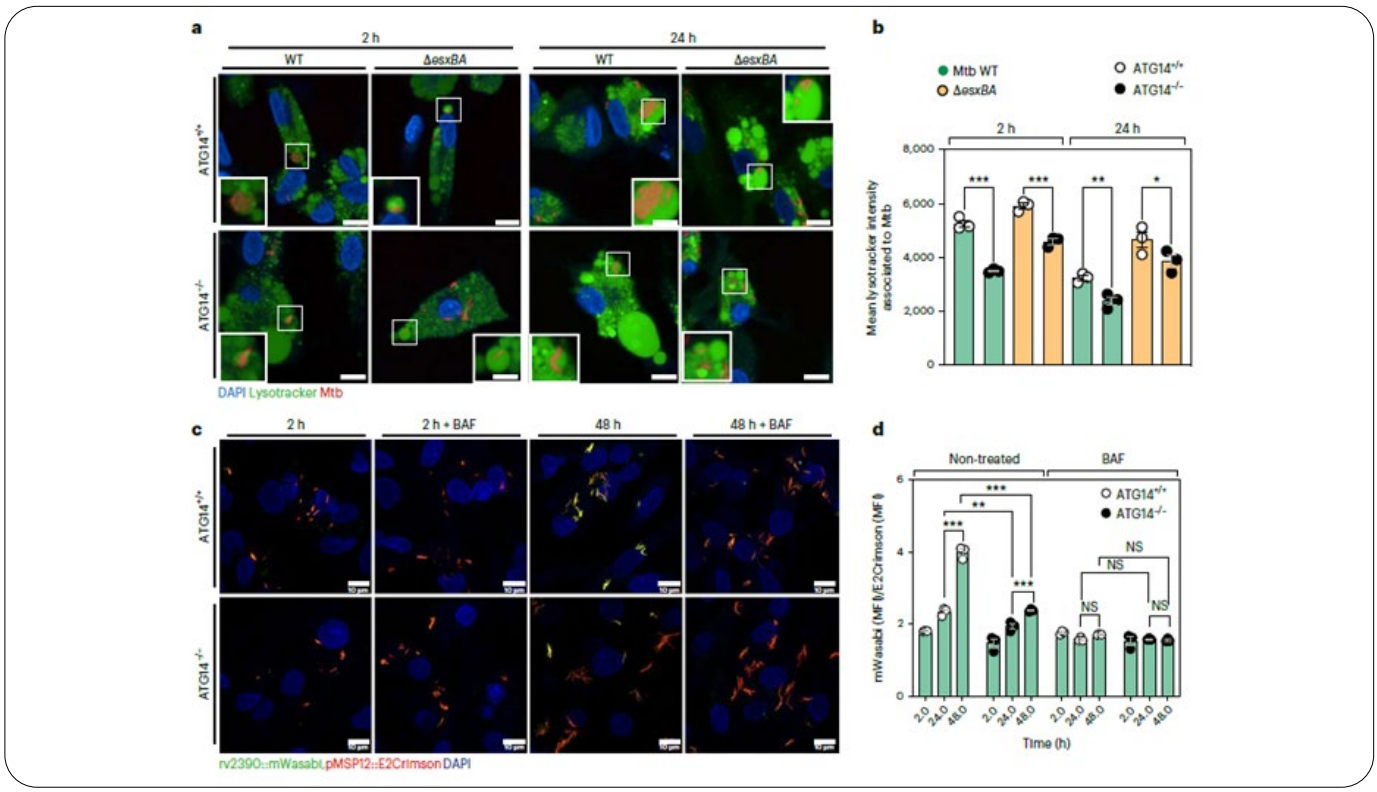

Figure 4: ATG14 is required for *Mtb* phagosome maturation. a) Snapshot of live ATG14$^{+/+}$ or ATG14$^{-/-}$ iPSDM infected with *Mtb* WT and Δ*esxBA* stained with LTR and NucBlue dye. Nuclear staining (blue), LTR (green), and *Mtb* E2-Crimson (red). Scale bars, 10 µm. b) Quantitative analysis of the LTR association with *Mtb* as mean fluorescence intensity. Data representative from one out of two independent experiments (n = 3 independent wells). Results are shown as mean ± s.e.m. One-way ANOVA followed with Šídák's multiple comparisons test. ***P < 0.001, **P < 0.002, *P < 0.033. Image credit: Aylan, Bernard, Pellegrino, et al., 2023

An unexpected finding of the study was the higher replication rate of *Mtb* Δ*esxBA* in ATG14 KO iPSDM, which is not able to efficiently access the cytosol. To explore this further, the team stained infected cells with an acidic organelle probe and quantified the fluorescence intensity to determine phagosome maturation. Two hours post-infection, the mean intensity was lower for both wild-type *Mtb* and Δ*esxBA* in ATG14 KO-infected iPSDMs and remained lower after 24 hours (Figure 4). Given that *Mtb* Δ*esxBA* is mostly found in phagosomes, the authors propose that ATG14 is therefore required for the maturation of *Mtb* phagosomes.

Conclusion

Last year, the World Health Organization (WHO) reported that the number of people infected with *Mtb*, including drug-resistant strains, had risen globally for the first time in almost 20 years. There is therefore an urgent need to uncover novel ways to treat *Mtb* infection and reduce the disease burden. Autophagy has recently emerged as an essential host immune defense mechanism against intracellular *Mtb* infection. However, the regulation and interaction between canonical (xenophagy) and non-canonical (LAP) autophagy responses during infection are poorly characterized in human macrophages.

By combining genetic knockout and high-content imaging approaches, the team confirmed that ATG7 and ATG14 are required to control *Mtb* infection by macrophages. They also identified specific roles for these proteins: ATG7 and ATG14 regulate the control of cytosolic *Mtb*, and ATG14 regulates the fusion of *Mtb* phagosomes with lysosomes. The authors conclude that understanding how autophagy acts to control the infection of intracellular pathogens in humans could enable the development of host-directed therapies in the future.

Reference

1. Aylan, B., Bernard, E.M., Pellegrino, E. et al. ATG7 and ATG14 restrict cytosolic and phagosomal Mycobacterium tuberculosis replication in human macrophages. *Nat Microbiol* (2023). https://doi.org/10.1038/s41564-023-01335-9

Revvity
940 Winter Street
Waltham, MA 02451 USA

(800) 762-4000
www.revvity.com

For a complete listing of our global offices, visit www.revvity.com
Copyright ©2023, Revvity. All rights reserved.